Identification of single-domain structures in the system YBa$_2$Cu$_3$O$_{7-\delta}$-Ag by magnetization measurements

F. Hanic, A. Cigáň, Š. Buchta, J. Maňka, V. Zrubec

Institute of Measurement Science, SAS, Dúbravská cesta 9, 842 19 Bratislava, Slovakia

Abstract

The magnetization methods were used in study of effect of Ag doping on the structural and superconducting parameters in two series of melted and highly textured samples of the system $(YBa_2Cu_3O_{7-\delta})_{1-x}(Ag_2O)_x$. The x concentration level of the first series ranged from 0 to 10 wt % and the second one from 0 to 3.6 wt % Ag$_2$O. By means of the SQUID magnetization measurements the optimum Ag$_2$O doping level ranged from 1.6 to 2.8 wt %. These methods led to optimization of conditions in preparation of single-domain samples. From the secondary precipitated CuO phase and from the appearance of Ag component the solubility limit of Ag in solid solution $YBa_2Cu_{3-y}Ag_yO_{7-y/2-\delta}$ was found.

1. Introduction

After discovery of new ceramic HT$_c$ superconductors a wide range of compounds was developed. Between them, the Y- and Bi-based systems are the most significant for practical applications. However, many of the physical, chemical or mechanical properties need to be improved. For YBa$_2$Cu$_3$O$_{7-\delta}$ (YBCO) superconductor many of the deficiencies can be solved by the silver adding. It accelerates the synthesis and the sintering processes in the system YBCO/Ag$_2$O. Silver enhances the mechanical toughness, the normal state electrical resistance and the thermal conductivity and causes a significant grain growth through the partial melting of the system. An important function of Ag (Ag$_2$O) additions is their ability to take up or to release oxygen and thus to facilitate the oxygen diffusion also in thick and dense samples of YBCO, where the diffusion is extremely sluggish. An effectual influence on the critical current density J_c and the grain quality of the interfaces has been reported. An important effect of Ag addition is the stabilization of YBCO against the atmospheric degradation influence. However, some important problems are not yet satisfactorily solved: formation of solid solutions, solubility of Ag in YBCO, the role of the silver excess in the (YBCO-Ag) ss and the role of the secondary precipitation of Ag due to the different solubility of the silver in the YBCO phase at high and low temperatures [1-5].

The main attention in this work is related to the previously mentioned problems. We shall try to find optimal parameters for formation of the single-domain samples depending on the Ag content.

2. Experimental

The bulk samples of $(YBa_2Cu_3O_{7-\delta})_{1-x}(Ag_2O)_x$ were prepared by solid state reaction of stoichiometric mixtures of oxides Y$_2$O$_3$, CuO, Ag$_2$O and BaCO$_3$. Figure 1 shows the processing conditions for the samples' preparation. The annealing process occurred in two steps. In the first one, decarbonization of the system took place at 1400 °C (20 min). In the next step the homogenized powder product containing stoichiometric amounts of silver in form of Ag$_2$O was pressed into pellets and sintered in O$_2$ atmosphere at 1150 °C for 60 min., slowly cooled from 1000 °C to 930 °C for 72 h and oxidized at 580 °C for 24 h. The phase composition was controlled by X-ray diffraction of the surface (XRDS) and by X-ray powder diffraction (XRPD). The microstructure was studied by polarized optical microscopy (OM), see Figures 2 and 3. The unit cell parameters were evaluated from XRPD and XRDB data obtained on a Philips PW 1710 generator and with CuKα radiation. The volume magnetization characteristics were measured by 2-nd order SQUID gradiometer by compensation method [6]. All magnetization characteristics of the samples were measured after zero-field cooling at 77.3 K in range of magnetic fields (10^{-1} - 10^5) A m^{-1}.
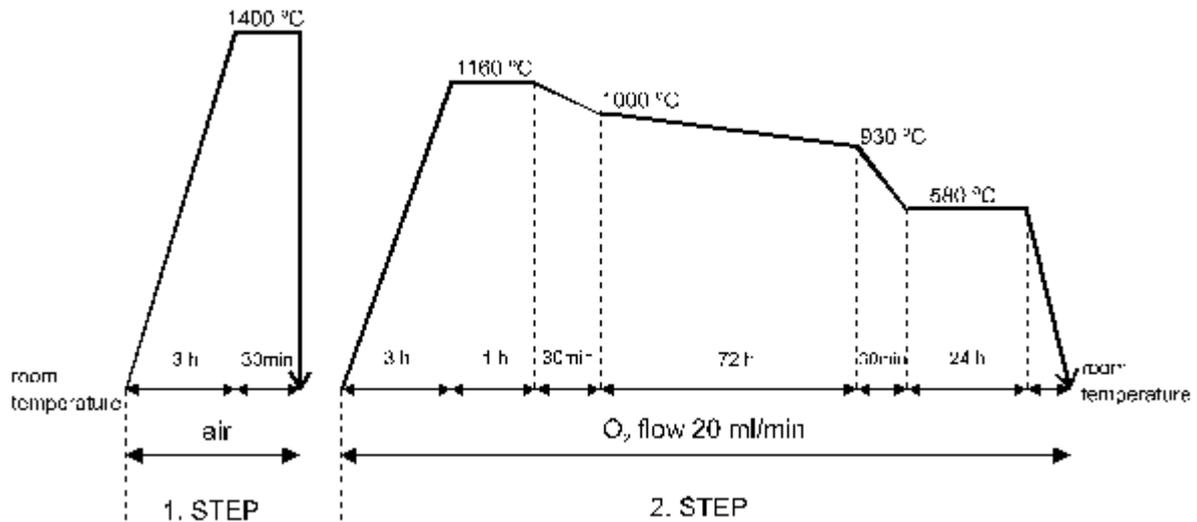
Figure 1. Diagram of processing conditions for the melt-growth process for preparation of textured samples in the system $(YBa_2Cu_3O_{7-\delta})_{1-x}(Ag_2O)_x$ with $x = 0.0 \div 10.0$ and $0.0 \div 3.6$ *wt* %.

a)   b)
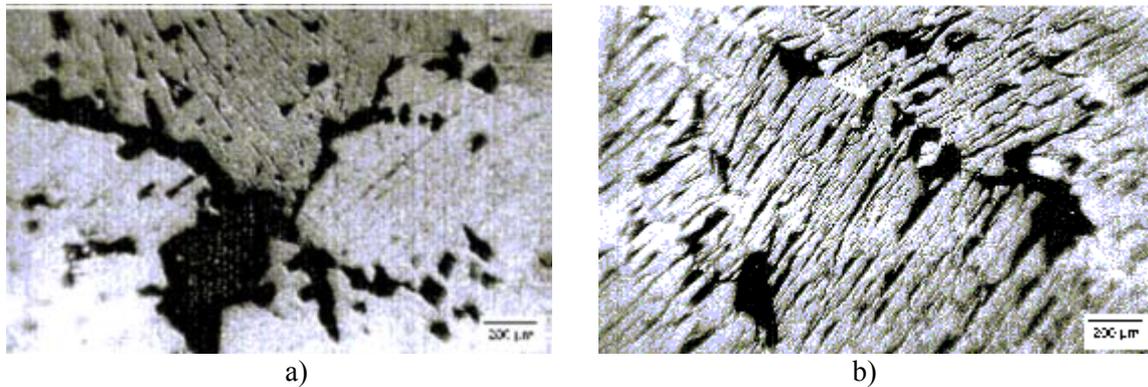
Figure 2. Polarized light micrograph of the melt-textured samples with the nominal composition $(YBa_2Cu_3O_{7-\delta})_{1-x}(Ag_2O)_x$.   a) $x = 0.0$,   b) $x = 1.6$.

a)   b)
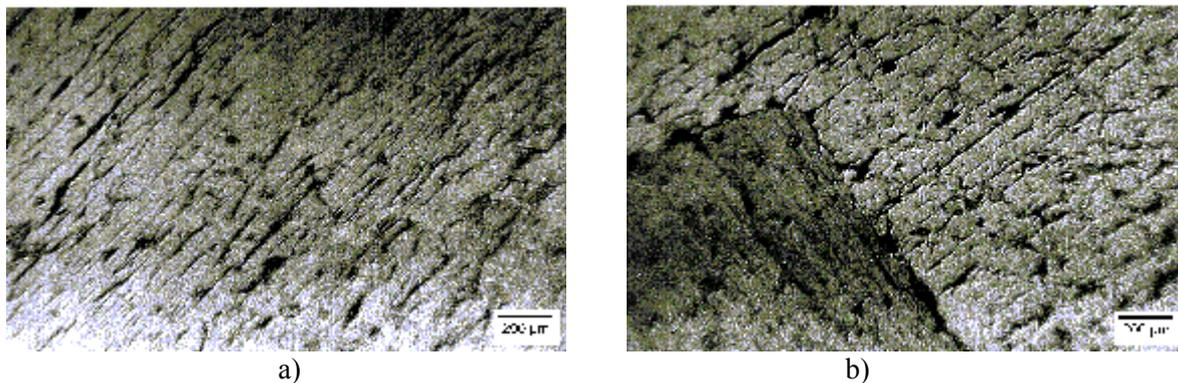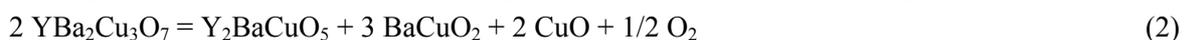
Figure 3. Polarized light micrograph of the melt-textured samples with the nominal composition $(YBa_2Cu_3O_{7-\delta})_{1-x}(Ag_2O)_x$ a) $x = 2.0$ b) $x = 2.8$.

3. Results and Discussion

Important indication about the substitution mechanism is given by the equation:

$$YBa_2Cu_3O_7 + y\, AgO_{0.5} = YBa_2Cu_{3-y}Ag_yO_{7-y/2} + y\, CuO + y/2\, O_2 \tag{1}$$

The appearance of CuO between reaction products has a competitive decomposition reaction:

$$2\, YBa_2Cu_3O_7 = Y_2BaCuO_5 + 3\, BaCuO_2 + 2\, CuO + 1/2\, O_2 \tag{2}$$

Also in the case, when both processes (eqs. 1 and 2) occur simultaneously, the molar fraction of CuO in the system should increase with increasing y. Reaching the solubility limit of Ag in YBCO (y_{lim}), the molar fraction of CuO begins to decline with the increasing y, since the excess amount of Ag, $y - y_{lim}$, remains in the system as a metallic silver.

The superconducting phase $YBa_2Cu_{3-y}Ag_yO_{7-y/2-\delta}$ in the surface of the samples is characterized by the different unit cell parameters in comparison with the parameters derived from the average powder data. The bulk density D_m and porosity P show continuous variation depending on the concentration x of the Ag_2O. The density D_m increases with the increasing x value, but porosity clearly shows a minimum in the range 1.6 to 2.8 wt % Ag_2O. The unit cell parameters and critical temperature T_c (89.4 K to 91.8 K) show only statistical but no systematic deviations within the concentration range $0 < x \le 3.6$ wt %.

AC magnetization M vs the applied field H_a for the first and second series of melt-textured samples with the nominal content x is shown in Figures 4 and 5. The results of the first group of samples (Fig. 4) show that the optimal doping level (as regards the porosity and superconducting properties) should be between $x = 1.0$ and 5.0 wt %. For this reason we prepared a new series of samples with concentration $x = 0.0$, 0.8, 1.2, 1.6, 2.0, 2.8, 3,6 wt %. AC magnetization loops of the second series are shown in Figure 5. It can be seen that the samples with silver oxide content $x = 1.6$
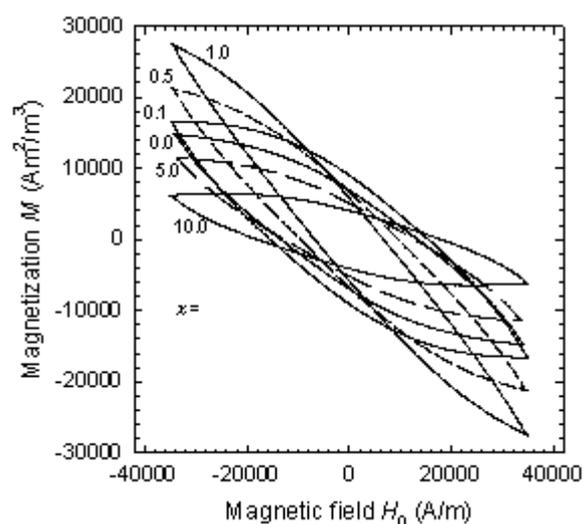

Figure 4. AC magnetization M vs the applied field H_o for the samples of the nominal composition $(YBa_2Cu_3O_{7-\delta})_{1-x}(Ag_2O)_x$, $x = 0.0$, 0.1, 0.5, 1.0, 5.0, 10.0 wt % (first series).
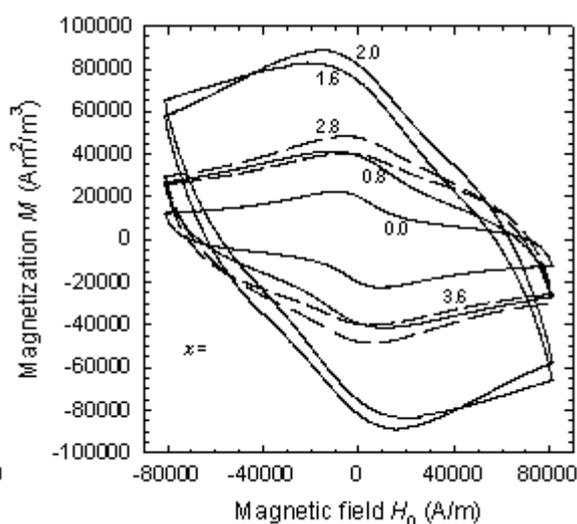
Figure 5. AC magnetization M vs the applied field H_o for samples of the nominal composition $(YBa_2Cu_3O_{7-\delta})_{1-x}(Ag_2O)_x$, $x = 0$, 0.8, 1.6, 2.0, 2.8, 3.6 wt % (second series).

and 2.0 have the best magnetization properties. The first magnetization peak corresponding to approximately zero applied field H_a can be related to the radius of shielding current loops of superconducting regions for our well textured samples. At low applied field the current loops are determined mainly by intergrain transport current properties. The higher magnetization peak the higher radius of shielding current loops can be expected, supposing that intragrain and also intergrain current properties do not change significantly. The addition of silver significantly supports grain growth, which is shown in Figures 2 and 3. The microstructure of the sample without silver addition shows multi-domain regions with well textured grains with cracks, presence of large pores and rather large and well resolved intergrain boundaries. The increasing of the silver doping results in lower porosity, decreasing intergrain disorientation and number of the domains. The sample with 2 wt % of Ag_2O has the best magnetization and shows presence of only one domain, Fig. 3a. The higher doping level increases multi-domain character, Fig. 3b, which is in full agreement with decreasing magnetization, Fig. 6. Diffraction data show single phase composition Y-123 for all investigated samples. It is in excellent agreement with optical microstructure (2D) and volume magnetization (3D) characteristics.

4. Conclusions

The highest magnetization hysteresis loops (Fig. 6) were found for the doping levels $x = 1.6$ and 2.0 *wt* %. We established the optimal Ag_2O doping level to be $x \cong 1.6$-2.8 *wt* %, at least in our processing conditions. In this interval the single-domain structure was created (see Fig. 3a) with the minimum porosity P. We did not observe the increase of the unit cell volume with Ag doping. The presence of the metallic Ag in the powdered samples of the second series with $x = 0.0$ to 3.6 *wt* % was not detectable. The XRDP phase analysis indicates a possible solubility limit of Ag in solid solution $YBa_2Cu_{3-y}Ag_yO_{7-y/2-\delta}$ to be $y_{lim} \sim 11$ *at* % Ag.

References

1. G. A. Costa, Paolo Mele, Intern. J. Modern Physics B, **13** (1999) 9&10, 1011.
2. B. Shao, A. Lin, Y. Z. Zhou, J. Zhang, J. Wang, Mat. Res. Bull. **24** (1989) 1369.
3. Ch. Zhang, A. Kulpa, A. C. D. Chaklader, Physica C **252** (1995) 67.
4. U. Wiesner, G. Krabbes, M. Ueltzen, C. Magerkurth, J. Plewa , H. Altenburg, Physica C **294** (1998) 17.
5. Y. Nakamura, K. Tachibana, S. Sato, T. Ban, S.I. Yoo, H. Fujimoto, Physica C **294** (1998) 302.
6. V. Zrubec, A. Cigáň, J. Maňka, Physica C **223** (1994) 90.